An experimental model for ice performance of podded propellers

Wang, J.; Akinturk, A.; Foster, W.; Jones, S. J.; Bose, N.

The 27th American Towing Tank Conference [Proceedings], 2004

27th American Towing Tank Conference
St. John's, Newfoundland and Labrador
Canada, August 6 and 7th, 2004

AN EXPERIMENTAL MODEL FOR ICE PERFORMANCE OF PODDED PROPELLERS

J. Wang / Memorial University of Newfoundland
A. Akinturk / Institute for Ocean Technology

W. Foster / Institute for Ocean Technology
S. J. Jones / Institute for Ocean Technology
N. Bose / Memorial University of Newfoundland

ABSTRACT

This paper describes the experimental model designed and built at Institute for Ocean Technology (IOT) to measure the ice performance of the podded propulsors in the ice tank. The model is capable of measuring forces and moments on the overall system, propeller shaft bearing loads and the loads on the blade during different operating conditions. Some results obtained from the ice tank testing are presented. Additionally, test conditions for ice performance are discussed.

INTRODUCTION

Recently, with the growing interest in the podded propulsors and with the increasing applications of this system, the number of icebreakers or ice-going vessels that have podded propulsors is increasing. As sea route developments and natural resource explorations in arctic or sub-arctic regions are increasingly carried out, the number of vessels capable of navigating in ice infested seas should be increased. Therefore, this paper presents the findings of the research carried out to investigate the performance of podded propulsors in ice conditions using ice tank experiments. Ice loads acting on the pod system were analyzed and the interactions between ice and propeller was considered.

An azimuthing pod system is a fully assembled propulsion unit and is also a steering unit without a general rudder. Inside the pod, there is an electric motor, which transfers power and signals from the ship through the strut. General benefits of podded propulsors are as follows: high steering ability, low level of noise and vibrations, increased payloads, lower operating cost, high ice going capability in astern direction, time saving during port calls and so on (Niini, 1997; Muller, 1999; Kron and Holmstrom, 1999; van Terwisga, 2001). There is some restriction of speed and power, however, which is caused by the capability and size of the electric motor and high manufacturing cost (Mewis, 2001).

So far, several experimental tests with model propellers had been carried out in the ice tank (Searle, 1999; Moores, 2002). These tests focused on ice loadings on the propeller blade, and the test results can be compared with those of this study. A few studies of podded propulsors in ice conditions have been performed (Niini, 1995; Juurmaa, 2001; Akinturk et al., 2004).

An azimuthing pod experimental model for this study consists of 0.95 meter long, 0.17 meter in diameter pod housing, 0.45 meter high streamlined strut and 0.3 meter propeller diameter. The ice tests were carried out at the IOT ice tank with various conditions. The open water tests were carried out in the same condition as ice tests. The EG/AD/S model ice (Timco, 1986) was used for these experimental tests.

NOMENCLATURE

- T Propeller Thrust
- Q Propeller Torque
- D Propeller Diameter
- r Propeller Radius
- P Propeller Pitch
- V Carriage Speed
- X X-Axis of Global Dynamometer
- Y Y-Axis of Global Dynamometer
- Z Z-Axis of Global Dynamometer
- X_a X-Axis of Aft Dynamometer
- Y_a Y-Axis of Aft Dynamometer
- Z_a Z-Axis of Aft Dynamometer
- X_b X-Axis of Blade Dynamometer
- Y_b Y-Axis of Blade Dynamometer
- Z_b Z-Axis of Blade Dynamometer
- X_f X-Axis of Forward Dynamometer
- Y_f Y-Axis of Forward Dynamometer
- Z_f Z-Axis of Forward Dynamometer
- K_T Thrust Coefficient

K_Q Torque Coefficient
F_X Force on X-Axis
F_Y Force on Y-Axis
F_Z Force on Z-Axis
M_X Moment on X-Axis
M_Y Moment on Y-Axis
M_Z Moment on Z-Axis
n Propeller Rotating Speed (Revolutions Per Second)
w Angular velocity
h_i Depth of cut

EXPERIMENTAL MODEL

Azimuthing podded propulsor model was designed and built at IOT for measuring forces and moments on each parts. In this experimental model, there are four six component dynamometers; (1) blade dynamometer at the root of one of the blades, (2) aft bearing dynamometer on the propeller drive shaft inside the pod, (3) fore bearing dynamometer on the propeller drive shaft inside the pod, (4) global dynamometer above the strut (Figure 1). These dynamometers measure the individual forces and moments acting at each position. In particular, the global dynamometer measures the global forces on the whole system: propeller, pod and strut.

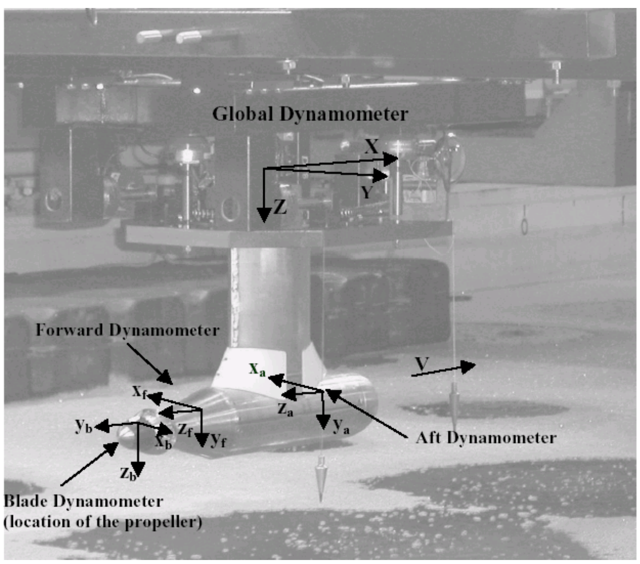

Figure 1: Assembled model with local axis

Depth of cuts, carriage speeds, propeller rotating speeds, azimuthing angles, and properties of the model ice were measured and recorded. Figure 2 shows the definition of depth of cut.

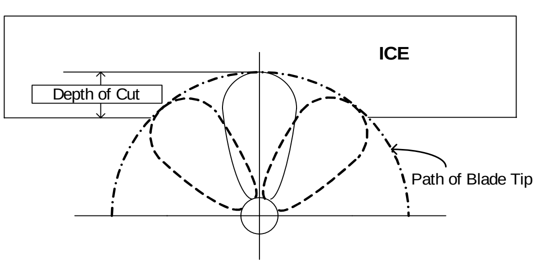

Figure 2: Definition of depth of cut

EXPERIMENTAL FACILITY

The tests were conducted in the ice tank at the National Research Council of Canada's Institute for Ocean Technology (Jones, 1987). The useable area of the tank for ice testing is 76 m long, 12 m wide and 3 m deep. In addition, a 15 m long setup area is separated from the ice sheet by a thermal door to allow equipment preparation while the test sheet is prepared (Figure 3). The range of the carriage velocity is from 0.0002 to 4.0 m/s. The carriage is designed with a central testing area where a test frame, mounted to the carriage frame, allows the experimental setup to move transversely across the entire width of the tank. All tests were recorded by four cameras; two were on the carriage, the others were under the water.

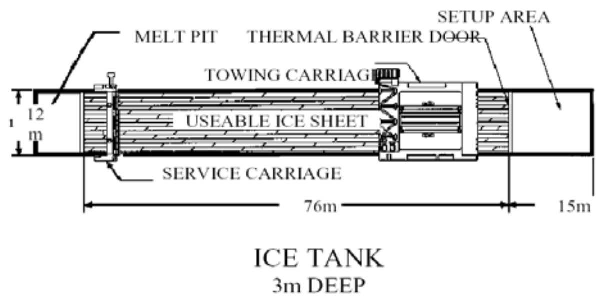

Figure 3: Schematic diagram of the ice tank

TEST PROCEDURE

There were four different tests: open water tests in tractor mode, open water tests in pusher mode, ice tests in tractor mode, and ice tests in pusher mode. Basically, each group of tests included three different propeller rotational speeds, two or three different carriage speeds, two different depths of cut, and different azimuthing angles from 0 to 180 degrees at 30 degrees intervals.

Ice tests were carried out with partially pre-sawn ice sheets (Figure 4) and pack ice (figure 5). Most ice tests were performed with 60 mm thickness of the ice and 80 kPa flexural strength of the ice. Several runs were tested with 80mm of ice thickness. During the tests, some of the data collection channels were saturated a few times (up to 3% of the total data points collected at the maximum). Table 1 shows the test matrix for this study.

Table 1: Test Matrix

Pod Mode	Tractor Mode, Pusher mode
Carriage Speed	0, 0.2, 0.5, 0.8 m/s
Propeller Rotating Speed	5,7,10 Hz
Depth of Cut	15mm, 35mm
Azim. Angle (Pusher Mode)	0, 30, 60degree
Azim. Angle (Tractor Mode)	180, 150, 120degree
Ice Condition	Pre-sawn Ice, Pack Ice
Ice Thick. / Flex. Strength	60mm / 80kPa

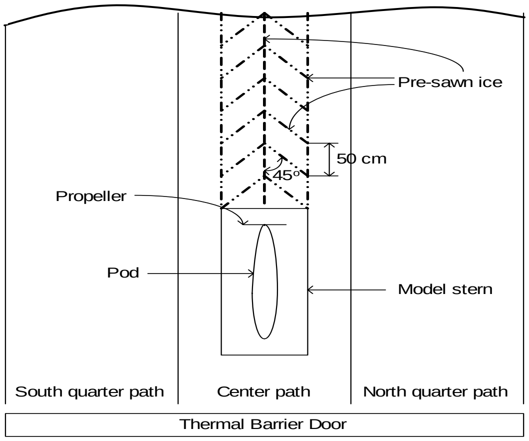

Figure 4: Sketch for Pre-sawn ice sheet

Figure 5: Pack Ice

MODEL ICE

Model EG/AD/S ice was used in these experiments. EG/AD/S ice is specifically designed to provide the scaled flexural strengths of the columnar sea ice (Timco, 1986). It is a diluted aqueous solution of ethylene glycol (EG), aliphatic detergent (AD), and sugar (S).

First, the ice sheet is grown by cooling the tank room to approximately -20 ^{o}C and then "seeding" the tank by spraying warm water into the cold air in a thin mist, allowing it to form ice crystals before it contacts the surface of the tank. The ice is then allowed to grow at approximately -20 ^{o}C until it has reached the desired thickness. The temperature of the room is then raised to above freezing and the ice is allowed to warm up and soften, a process called tempering, until the target ice strength is reached.

TEST RESULTS

Some of the test results are presented in this section. The test condition was 60 mm thickness, pre-sawn ice with 35 mm depth of cut in the tractor and pusher mode. Pack ice tests and open water tests were carried out at the same conditions as the pre-sawn ice tests. Figure 6 and figure 7 show the azimuthing angle and operating conditions for tractor mode.

Figure 8 and figure 9 show the non-dimensional average thrust coefficient (K_T) and ten times torque coefficient (10*K_Q) in the tractor mode as a function of advance coefficient (*J*) for both pre-sawn ice and open water conditions with three different azimuthing angles: 180, 150, 120 degrees.

These figures show the ice contact resulted in increased values of the thrust and torque coefficients over open water values corresponding to advance coefficient *J*. Some reasons are due to the wake of the ice (blockage effects) proximity effects. The milling loads may help to increase the thrust and torque coefficient as well. If the milling loads are acting on the pressure side of the blade (Kotras et al., 1985), the thrust coefficients are increased.

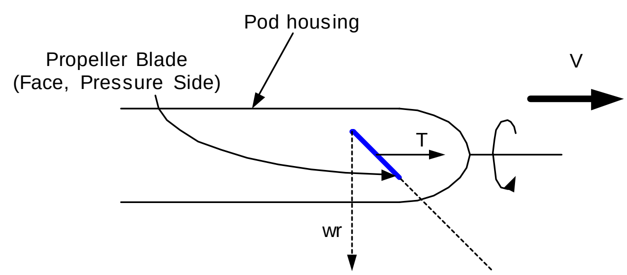

Figure 6: Tractor mode with 180 degrees azimuthing angle

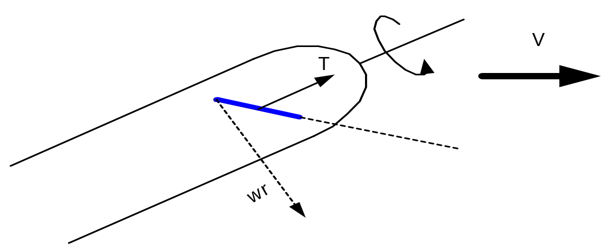

Figure 7: Tractor mode with 150 degrees azimuthing angle

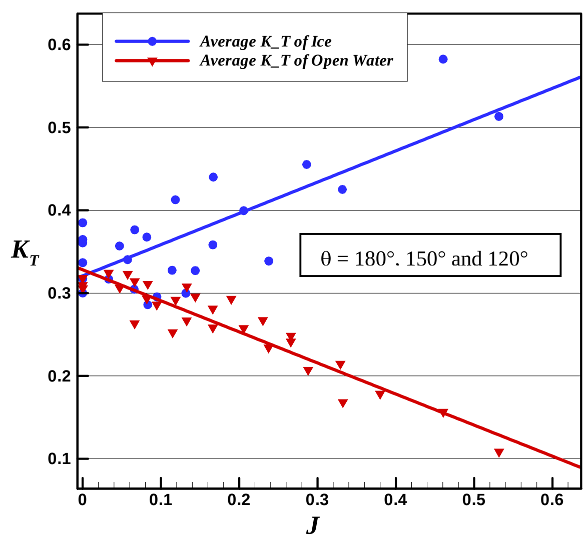

Figure 8: K_T versus *J* (Tractor Mode)

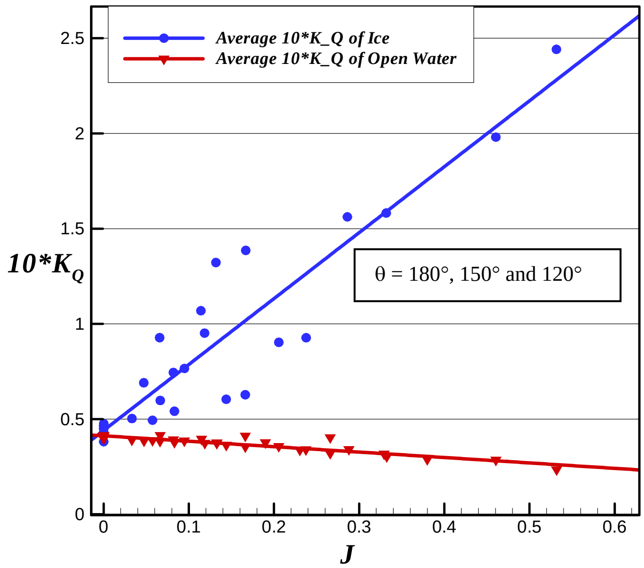

Figure 9: ***10*K$_Q$*** **versus** ***J*** **(Tractor Mode)**

Figure 10 and figure 11 show the azimuthing angle and operating condition for pusher mode. Figure 12 and Figure 13 show the non-dimensional average thrust coefficient (K_T) and ten times torque coefficient (10*K_Q) in the pusher mode as a function of advance coefficient (J) for both pre-sawn ice and open water conditions with three different azimuthing angles: 0, 30, 60 degrees.

In case of the pusher mode, propeller was placed behind the pod. Therefore, broken ice pieces hit the propeller blade randomly. This caused the wide range of scatter, but overall trend is similar to the open water results.

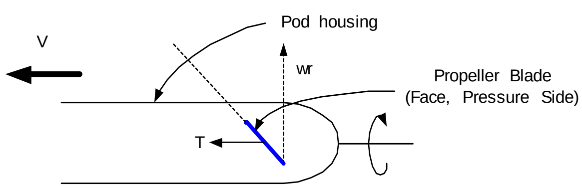

Figure 10: Pusher mode with 0 degree azimuthing angle

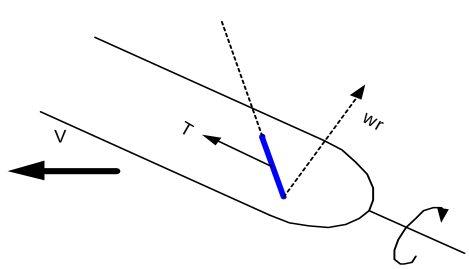

Figure 11: Pusher mode with 30 degrees azimuthing angle

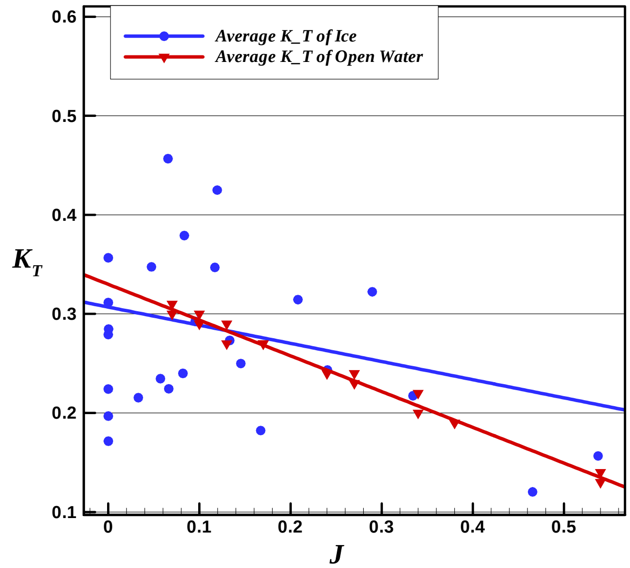

Figure 12: ***K$_T$*** **versus** ***J*** **(Pusher Mode)**

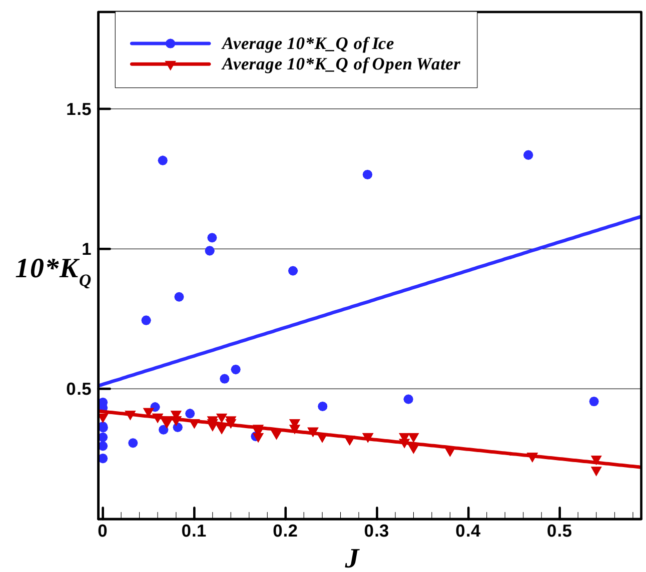

Figure 13: ***10*K$_Q$*** **versus** ***J*** **(Pusher Mode)**

The effect of azimuthing angles on the thrust coefficient for both tractor and pusher mode is plotted in figure 14 and figure 15, in which average values are provided. As the angle from centerline of the pod was increasing, thrust coefficient values were increasing too. In figure 15, the propeller in the 60-degree of azimuthing angle for pusher mode experienced unbroken ice.

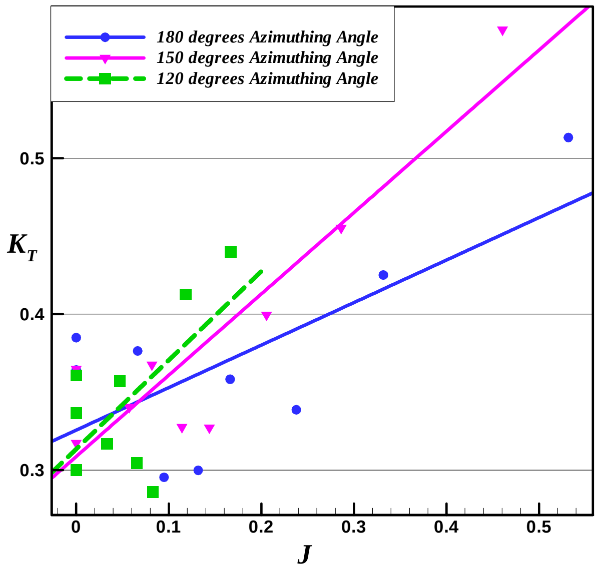

Figure 14: Effect of azimuthing angle on K_T for tractor mode

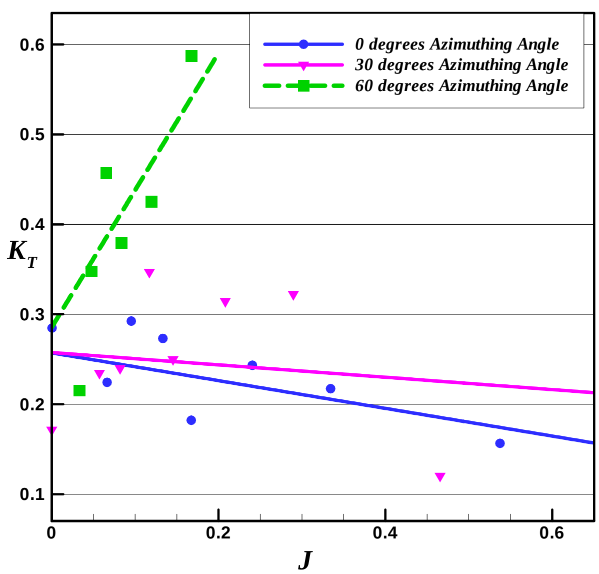

Figure 15: Effect of azimuthing angle on K_T for pusher mode

Figure 16 shows the non-dimensional global force F_X as a function of the advance coefficients, and Figure 17 shows the raw data with carriage speed and RPS. The global force F_X indicated the sum of the propeller wake forces and the drag (resistance) acting on the whole unit. The values of F_X are scattered over a plot area, especially at a low advance coefficient region. The reason is that this plot contains three different azimuthing angles that are 180, 150 and 120 degrees for tractor mode.

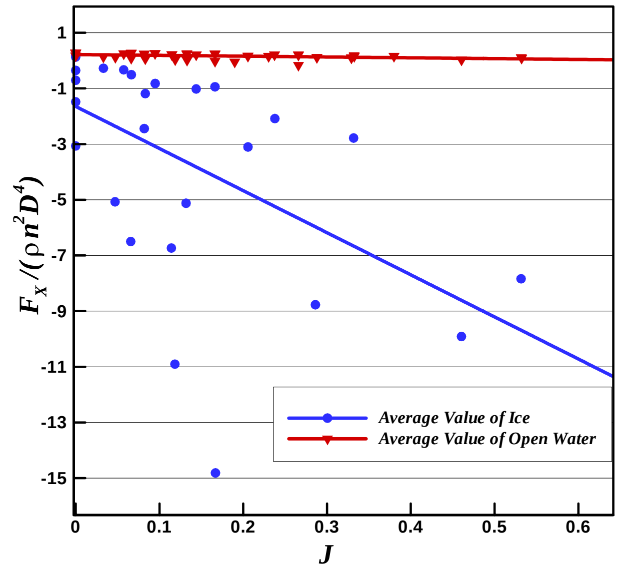

Figure 16: Non-dimensional global F_x versus J

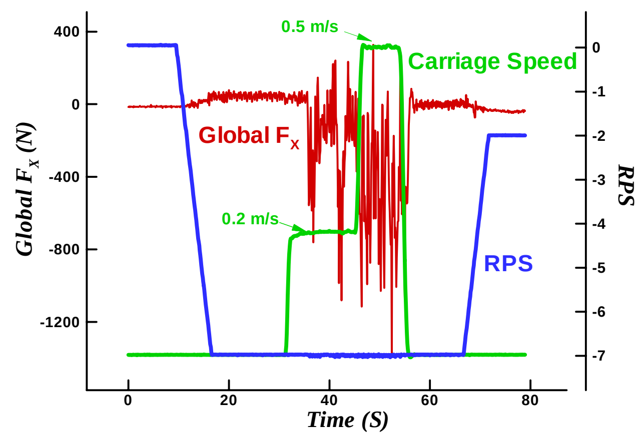

Figure 17: Global F_X, Carriage speed and RPS

Figure 18 shows the effect of azimuthing angle on the non-dimensional global force F_X. When the azimuthing angle is decreasing, the magnitude of F_X is increasing. The reason is that the contact area between the pod and the ice is getting wide at the lower azimuthing angle.

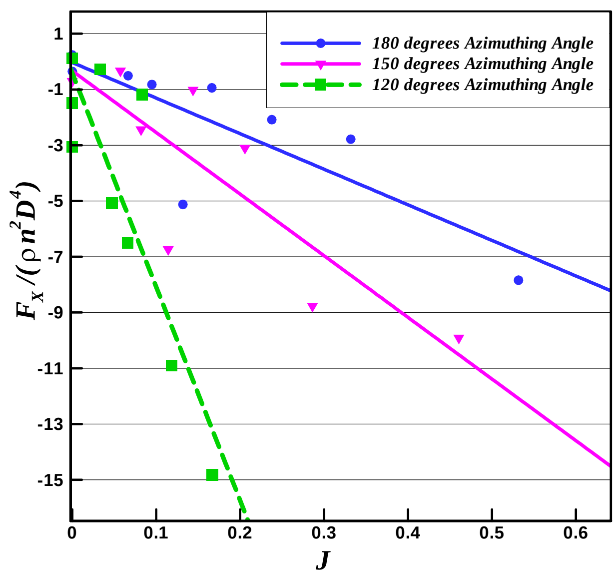

Figure 18: Effect of azimuthing angle on global F_X for tractor mode

Figure 19 shows the global force F_X for pre-sawn ice, pack ice and open water simultaneously during one revolution of the propeller. Usually, the largest F_X of global force was found at the pre-sawn ice. As the pack ice, however, had its own acceleration and random direction to act on the blade, sometimes pack ice had the maximum value among them.

Number of peak is equal to the number of blade. When the propeller blades enter the ice block, loads reach the maximum value.

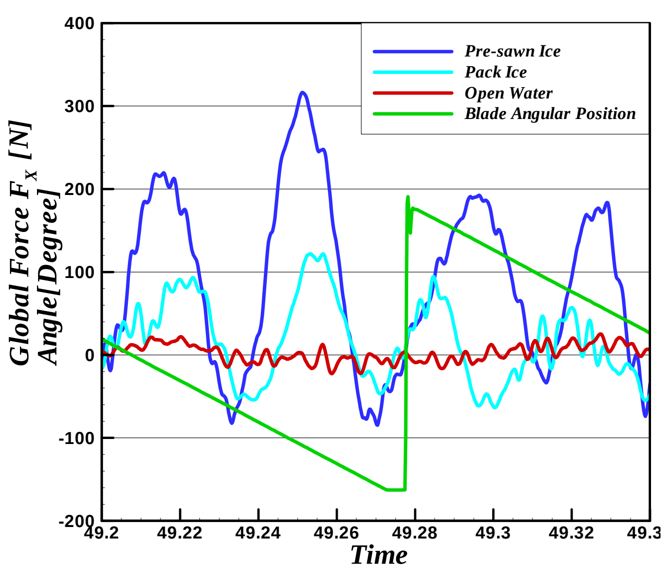

Figure 19: Global F_X comparison among pre-sawn ice, pack ice and open water during one propeller revolution

Figure 20 and Figure 21 show the effect of depth of cut and propeller rotating speed on the shaft torque. As depth of cut is higher, the shaft torque is higher. However, propeller rotating speed is higher, shaft torque is lower.

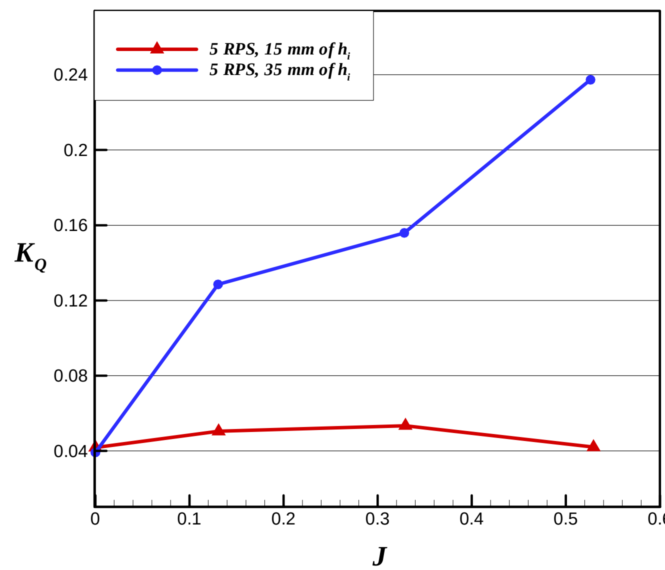

Figure 20: K_Q versus J with two different depth of cut at 5 RPS

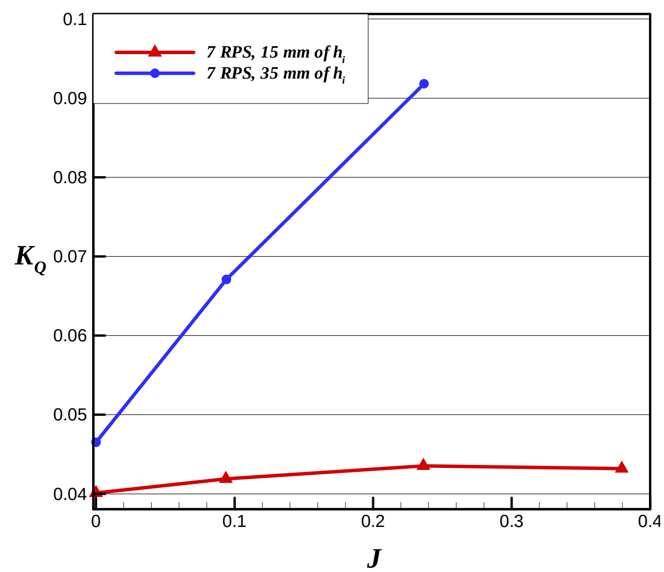

Figure 21: K_Q versus J with two different depth of cut at 7 RPS

CONCLUSION

This experimental study explained the characteristics of podded propulsors in ice conditions. The design and operating criteria for ice interacted podded propulsors can be suggested. Knowledge obtained in this study can also be utilized to update regulations for ice class propellers.

ACKNOWLEDGMENTS

The study on the podded propellers is a joint project between Transport Canada and the National Research Council of Canada. Furthermore, thanks are due to Memorial University's Technical Services Department for their help in the experimental work. Special thanks are extended to the members of the NRC- IOT for their assistance in various stages of this project.

REFERENCES

Akinturk, A., Jones, S., Rowell, B., Duffy, D. (2004), "Measuring Podded Propeller Performance in Ice", Proceedings of the 1st International Conference on Technological Advances in Podded Propulsion, Newcastle, UK.

Jones, S. (1987), "Ice Tank Test Procedure at the Institute for Marine Dynamics", Report No. LM-AVR-20, Institute for Ocean Technology, National Research Council of Canada.

Juurmaa, K., Mattson, T. and Wilkman G. (2001), "The Development of the New Double Acting Ships for Ice Operation", 16th International Conference on Port and Ocean Engineering under Arctic Conditions (POAC'01), Ottawa.

Kotras, T., Humphreys, D., Baird, A., Morris, G. and Morley, G. (1985), "Determination of Propeller-Ice Milling Loads", Proceedings of the Fourth International Offshore Mechanics and Arctic Engineering Symposium, Vol. 2, pp.336-343, Dallas.

Kron, P. and Holmstrom, L. (1999), "Hydrodynamic Aspects of Mermaid Propulsion System", 21st Century Cruise Ship, London/IMARE conferences and symposia, Vol. 111, No.3.

Mewis, F. (2001), "The Efficiency of Pod Propulsion", Proceedings of the 22nd International Conference on Hydrodynamics and Aerodynamics in Marine Engineering, Bulgaria.

Moores, C. (2002), "Shaft and Blade Load Measurements on a Highly Skewed Propeller Model in Ice" Master of Engineering Thesis, Memorial University of Newfoundland, St. John's, Newfoundland.

Muller, J. (1999), "Podded Drives and Conventional Cargo Tonnage", 21st marine propulsion conference, Athens.

Niini, M. (1995), "New Propulsion Technology for Arctic Tankers", Shipbuilding Technology International.

Niini, M. (1997), "Azipod Propulsion Breakthrough for Large Cruise", Cruise & Ferry, London.

Searle, S. (1999), "Ice Tank Test of a High Skewed Propeller and a Conventional Ice-Class Propeller in Four Quadrants", Master of Engineering Thesis, Memorial University of Newfoundland, St. John's, Newfoundland.

Timco, G. (1986), "EG/AD/S: A New Type of Model Ice for Refrigerated Towing Tanks", Cold Science and Technology, Vol. 12, pp. 175-195.

van Terwisga, T., Quadvlieg, F. and Valkhof, H. (2001), "Steerable Propulsion Units: Hydrodynamic issues and Design Consequences", Occasion of the 80th anniversary of Schottel GmbH & Co.